# High Performance PEEK/AlN Micro- and Nanocomposites for Tribological Applications

**R. K. Goyal,[1] A. N. Tiwari,[2] Y. S. Negi[3]**

[1]*Department of Metallurgy and Materials Science, College of Engineering, Shivaji Nagar, Pune 411 005, India*
[2]*Department of Metallurgical Engineering and Materials Science, Indian Institute of Technology, Bombay, Powai, Mumbai 400 076, M.S., India*
[3]*Polymer Science and Technology Laboratory, Department of Paper Technology, Indian Institute of Technology, Roorkee, Saharanpur Campus, Saharanpur 247 001, U.P., India*

Received 28 May 2010; accepted 29 April 2011
DOI 10.1002/app.35567
Published online 6 December 2011 in Wiley Online Library (wileyonlinelibrary.com).

**ABSTRACT:** The tribological properties of poly(ether–ether–ketone) (PEEK)/aluminum nitride (AlN) composites reinforced with micro- and nano-AlN particles were evaluated under dry sliding conditions. The wear resistance of pure PEEK is 10-fold higher than mild steel. It was further improved by 2-fold at 20 wt % micro-AlN and by more than 4-fold at 30 wt % nano-AlN composite compared with pure PEEK. The improvement in wear resistance was attributed to a thin and coherent transfer film. However, it was deteriorated on further increasing micro-AlN. The coefficient of friction of the composites was increased. Scanning electron microscopy and optical microscopy of worn surfaces and transfer films have been explained in detail. © 2011 Wiley Periodicals, Inc. J Appl Polym Sci 124: 4612–4619, 2012

**Key words:** composites; wear; friction; PEEK; AlN

## INTRODUCTION

High performance polymer composites[1,2] are used increasingly for engineering applications under hard working conditions. They provide unique mechanical, thermal, and tribological properties with low weight to ensure safety and economic efficiency. For examples, plastic gears are widely used for the parts of copy machines and printers due to light weight, reduced noise, anticorrosion, and an excellent flexibility in design when compared with metal gears.[3] In tribological environment, the virgin polymer could not be used due to its higher coefficient of thermal expansion (CTE) and low thermal conductivity. This results in transfer film layers of lower thermal conductivity between the meeting surfaces. In other words, the contact temperatures are higher and may frequently reaches near to the melting temperature of the matrix.[4] New developments in the automotive sector demand for the polymer composites, which can withstand higher loads and environmental temperature of about 120°C.[5] Under such conditions, polyamide and ultra high molecular weight polyethylene could not fulfill the requirements completely.[6]

Although the addition of fillers to polymers improved their hardness, stiffness, and strength, which resulted in improved wear resistance.[7] However, the hardness[8] and strength[9] are not only the factors controlling the wear behavior but also the nature and stability of the transfer film developed between the sample and counterface, and its adhesion to the counterface affects the wear properties.[10,11] The transfer film mainly consists of worn fillers and matrix fragments, which could reduce the direct contact between the sample and counterface. This may lead to decrease in the contact pressure and the sub-surface stress. Under such circumstance the wear resistance is increased provided the transfer film is thin, uniform, and tenacious.[12,15] Lancaster et al. demonstrated that the wear rate of composites is reduced by modifying the counterface surface and by supporting the applied load.[12] Wear resistance of PTFE composites have been improved by more than two orders of magnitude by reinforcing alumina[16] and ZnO nanofillers. However, friction coefficient was higher than the unfilled PTFE.[17] Nevertheless, addition of fillers such as ZnO and SiC to polyphenylene sulfide[9] and CuO, CuS, and $CuF_2$ to poly(ether–ether–ketone) (PEEK)[11,15] deteriorated the wear resistance of pure polymer due to the poor adhesion of the transfer film with the counterface. Moreover, the wear resistance significantly depends on other factors such as dispersion state, size, volume, and type of filler particles,[18,19] surface roughness of the countersurface,[20] and crystallinity of the polymer.[19] On the other hand, coefficient of friction does not depend on the type[21] and size[13] of filler particles.

*Correspondence to:* R. K. Goyal (rkgoyal72@yahoo.co.in).

PEEK has been widely used in many applications due to its unique properties such as outstanding thermal, mechanical, chemical, moisture resistant properties, low coefficient of friction, and high service temperature.[22,23] It is an attractive material for journal bearings and piston rings under various loading conditions as it is comparatively fatigue resistant and exhibits a low creep rate up to about 250°C.[24,25] Despite its low coefficient of friction, its wear resistance often limits its utilization in tribological system. The specific wear rate of PEEK was quoted to be about $10^{-5}$ $mm^3/N$ m, which appear to be too large to be used as a rubbing surface material in machinery.[4] However, its wear resistance can be significantly enhanced by up to two orders of magnitude by introducing fillers such as carbon fiber,[24] carbon nanofibers,[25] short carbon fibers,[26] CuS,[13] $Si_3N_4$,[14] $SiO_2$,[15] SiC,[27] and $ZrO_2$.[28] The improved wear resistance was attributed to the smoothing of the counterface, and the developing of a transfer film which results in reduced ability for ploughing, tearing, and other non-adhesive components of wear. Plasma surface treatment improved the wear resistance of PEEK and its composites due to cross linking of PEEK and improvement of the interface strength of composites.[7]

Recently, we have demonstrated that micro- and nano-size aluminum nitride (AlN) particles are very effective in improving the thermal, crystallization, mechanical, and dielectric properties of PEEK.[1,2,29] It is well known that AlN is widely used as electronic substrates, heat sinks, and electronic packaging due to its low CTE ($4.4 \times 10^{-6}$/°C), high electrical resistivity ($>10^{14}$ Ω cm), high thermal conductivity (230 W/m K), and low dielectric constant (8.9 at 1 MHz).[30] Despite its good thermal, mechanical and electrical properties, unfortunately tribological properties of AlN filled polymer composites were rarely reported in literature. It was, therefore, thought to be worthwhile to explore the effect of the AlN on the wear and friction properties of PEEK. Moreover, it is expected that owing to good thermal conductivity of AlN (better than $Si_3N_4$, $SiO_2$, SiC, and $ZrO_2$), this might improve wear resistance of polymer composites. For this purpose, PEEK matrix composites reinforced with 0–50 wt % micro-AlN and 0–30 wt % nano-AlN particles were prepared by hot pressing and their wear and friction properties were evaluated using pin-on-disk wear tester.

## EXPERIMENTAL

### Materials

The commercial PEEK (GATONE™: Grade 5300PF) was used as matrix. It has a reported inherent viscosity of 0.87dl/g measured at a concentration of 0.5 g/dl in $H_2SO_4$. The particulate AlN powder supplied by Aldrich Chemical Company was used as received. As received ethanol of Merck make was used for homogenizing the AlN and PEEK mixture. Particle size distribution for the PEEK and AlN were determined on a GALAI CIS-1 laser particle size analyzer. The particle size of PEEK powder ranges from 4 to 49 μm and of AlN from 1.5 to 9.6 μm. The mean diameter of the PEEK particle was 25 μm and of the AlN was 4.8 μm. The particle size of nano-AlN powder obtained from Alfa Chemical Company was 10–20 nm.

### Preparation

High performance PEEK matrix composites reinforced with 0–50 wt % micro-AlN and 0–30 wt % nano-AlN were prepared using hot compression molding. PEEK and AlN powder were dried overnight in an oven at 150°C. Dried powder of micro-AlN and PEEK was well premixed in an ethanol medium through magnetic stirring in concurrent with heating to evaporate ethanol. In case of nanocomposites, dried nano-AlN powder was suspended in an ethanol for 3 h under ultrasonic bath to break down the agglomerates before mixing with PEEK powder. Except additional step of ultrasonication, remaining procedure was similar for both systems. Simultaneous stirring and heating will not allow settling of AlN particles at the bottom of the beaker. The suspension was stirred continuously at 80°C for 8 h on a digital magnetic stirrer [Heidolph MR 3001 K], which results in PEEK/AlN powder. The resultant powder was dried in an oven at 120°C to remove an ethanol. Then, the pure PEEK and its composite samples were prepared using a laboratory hot press under a pressure of 15 MPa and 350°C. Composite samples were coded by ANM-X and ANN-X, where ANM and ANN denote micro-AlN and nano-AlN powder, respectively as reinforcement in the PEEK matrix. The $X$ is the wt % of micro- or nano-AlN powder in the matrix. Table I shows wt % and vol % of AlN particles added to the PEEK matrix. The weight fraction of AlN can be changed to volume fraction by using equation; $V_f = W_f/[W_f + W_m(\rho_f/\rho_m)]$, where $V_f$ is the volume fraction, $W_f$ is the weight fraction, and $\rho_f$ is the density of AlN particles. $W_m$ and $\rho_m$ are the weight fraction and the density of PEEK matrix, respectively.

### Characterization

Wear rate and coefficient of friction were conducted on a pin-on-disk wear tester at a sliding speed of 1.0 m/s and nominal pressure of 0.5–1.25 MPa. The tests were conducted for a total sliding distance of 9 km, which were divided into three stages with

**TABLE I**
**Weight (Volume) Percentage of AlN Particles Added to the PEEK Matrix**

| | | | | | |
|---|---|---|---|---|---|
| wt % | 10 | 20 | 30 | 40 | 50 |
| vol % | 4.21 | 9.00 | 14.50 | 20.9 | 28.4 |

wt % AlN into vol % was converted by assuming the density of PEEK and AlN 1.29 and 3.26 g/cm$^3$, respectively.

3 km each cycle. The EN-24 steel (C: 0.4 %, Si: 0.2 %, Mn: 0.6 %, Ni: 1.5 %, Cr: 1.2 %, Mo: 0.3 %, and Fe: bal.) disk of diameter 76.48 mm and 5 mm thick was used as a countersurface. It was heat treated to harden to $R_c$ 50–52. The disk surface was abraded with water proof SiC paper to a surface roughness of $R = 0.06$ μm. The surface of the countersurface and pin was cleaned thoroughly with cotton dipped in acetone. The test was performed under a 48 ± 2 relative humidity and 30°C condition. The specific wear rate ($W_s$) can be determined by the slop of the line between the height loss per unit sliding distance ($h/s$) and the nominal pressure ($p$) as given in Eq. (1).[31]

$$h/s = W_s p$$

where $h$ is the height of the sample removed and $s$ is the sliding distance. The composite pin height losses were measured by measuring height to an accuracy of 1 μm. To investigate the role of transfer film on wear rate, the specific wear rate of mild steel (MS) was also determined under the similar test conditions.

Scanning electron microscopy (SEM) (Philips XL-30) was used to examine the worn surface of the composites pins and wear debris. All samples were coated with a thin layer of gold to make them electrically conductive prior to examining on SEM. Energy dispersive spectroscopy (EDS) was used to test the elemental composition of the contact surface of the composites. The transfer films formed between the pin and countersurface were examined by optical microscopy.

## RESULTS AND DISCUSSION

### Wear and friction testing

Figure 1 shows the specific wear rate ($W_s$) for the MS, PEEK, and PEEK/AlN microcomposites. The $W_s$ of PEEK is 9.7 × 10$^{-6}$ mm$^3$/N m and of MS is 95 × 10$^{-6}$ mm$^3$/N m under the similar test condition. The $W_s$ of MS is approximately one order of magnitude higher than that of pure PEEK despite its much higher Vickers hardness (125 kg/mm$^2$) compared with PEEK (24 kg/mm$^2$). It may be due to the formation of hard iron oxides debris during repeated

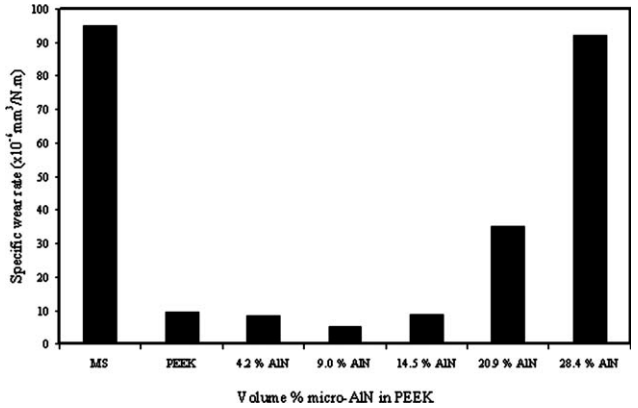


**Figure 1** Specific wear rate for mild steel (MS), PEEK and PEEK/AlN microcomposites (sliding speed: 1 m/s and sliding distance: 9 km). Data show the average of three readings.

sliding and hence, poor transfer film on the countersurface. In addition to this, for steel–steel sliding, the main factor may be attributed to adhesive wear due to the cold welding points. In case of pure PEEK, moderate wear rate is attributed to the unstable transfer film appeared on its wear scar which results in lumpy and flaky debris. These debris particles could not be spread out uniformly and hence resulting in poor adhesion between the transferred debris and countersurface.[11] Figure 2 shows the $W_s$ for the MS, PEEK, and PEEK/AlN nanocomposites. It can be seen from Figures 1 and 2 that the $W_s$ of the micro- and nanocomposites decreases with increasing AlN content and it reaches to a minimum level, i.e., 5.2 × 10$^{-6}$ mm$^3$/N m for 20 wt % (9 vol %) micro-AlN composite and 2.3 × 10$^{-6}$ mm$^3$/N m for 30 wt % (14.5 vol %) nano-AlN composites. When the micro-AlN content is above 30 wt %, the $W_s$ is increased drastically with an increasing AlN content, despite their higher hardness and stiffness[1,2] compared with pure PEEK. The significant improvement

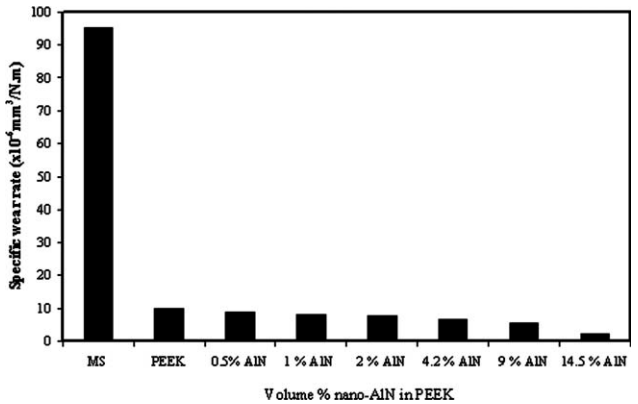


**Figure 2** Specific wear rate for mild steel (MS), PEEK, and PEEK/AlN nanocomposites (sliding speed: 1 m/s and sliding distance: 9 km). Data show the average of three readings.

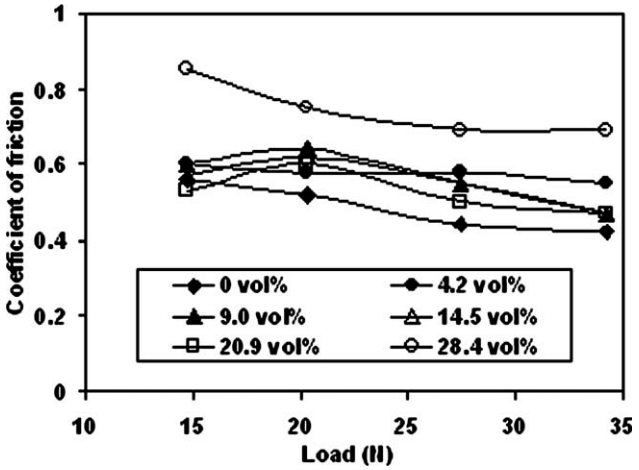


**Figure 3** Coefficient of friction as a function of load for PEEK/AlN microcomposites (sliding speed: 1 m/s and sliding distance: 9 km).

in wear resistance (inverse of specific wear rate) of composites may be attributed to two main factors. First, the increased hardness and stiffness of the composites containing lower wt % AlN. Second, formation of a thin, uniform, and tenacious transfer film on the counterface. This transfer film covers the asperities of the counterface and reduces its wearing effect on the composite pin surface. The resultant transfer film plays the dominant role during wear process. The decreased wear resistance at higher micro-AlN content may be attributed to several factors. First, poor quality transfer film could not cover the asperities of counterface. Second, poor quality transfer film results in decrease in interparticle distance of detached micro-AlN particles in the transfer film with increasing micro-AlN particles which in turn leads to aggregation of AlN particles. These aggregates may act as additional abrasives and give rise to birth to a third body wear mechanism. The resultant debris was powdery and separated out from the countersurface during subsequent sliding because of poor adhesion to the countersurface. Third, angularity shaped hard micro-AlN particles may substantially abrade the countersurface, as verified by examining the worn surface of 50 wt % (28.4 vol %) composite pin using EDS, and regenerate new track during every successive cycle, which results in additional wear of the composite. To understand the wear mechanism of composites SEM, EDS and optical microscopy of the composite samples have been discussed in next section.

Figures 3 and 4 show the coefficient of friction ($\mu$) of the PEEK/AlN micro- and nanocomposites, respectively as a function of load and AlN loading. From Figure 3, it can be seen that the $\mu$ for pure PEEK decreases with increasing load. The $\mu$ for micro- and nanocomposites was also decreased slightly with increasing load. However, it is clear that the $\mu$ of all microcomposites was higher than that of pure PEEK. This is similar to the results of PTFE composites containing Ni powder.[8] For the 50 wt % microcomposite, the $\mu$ was highest and fluctuated between 0.69 and 0.85. However, the $\mu$ or nanocomposites was slightly lower at smaller load and higher at larger load than that of pure PEEK as shown in Figure 4. The higher $\mu$ may be attributed to the increased contribution to the deformation components of friction by the hard AlN particles during sliding against the polymer and similar particles present in the transfer film.[11]

### Optical microscopy of the transfer films

Figure 5(a) shows optical microscopy image of as polished initial surface of the countersurface. Figure 5(b–d) shows the transfer films developed after 3 km sliding by pure PEEK, 20 wt % and 50 wt % microcomposites, respectively. Figure 5(b) shows that pure PEEK forms a transfer film with moderate quality, which does not cover completely trough and asperities of the countersurface. In case of 20 wt % microcomposite, formation of a uniform and tenacious transfer film occurs as shown in Figure 5(c). This contributes to a significant decrease in specific wear rate. But, in case of 50 wt % microcomposite, there is only partial development of transfer film on the countersurface as shown in Figure 5(d,e). This may be due to the poor adhesive strength of the transfer film with countersurface.[8] It is well known that at higher ceramic particles loading particle–particle interaction occurs, which results in aggregates. Hence, these aggregates hinder the formation of a continuous transfer film on the countersurface.

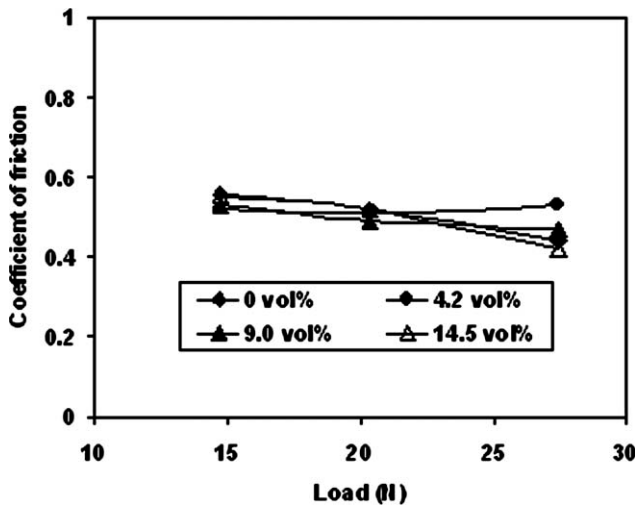


**Figure 4** Coefficient of friction as a function of load for PEEK/AlN nanocomposites (sliding speed: 1 m/s and sliding distance: 9 km).

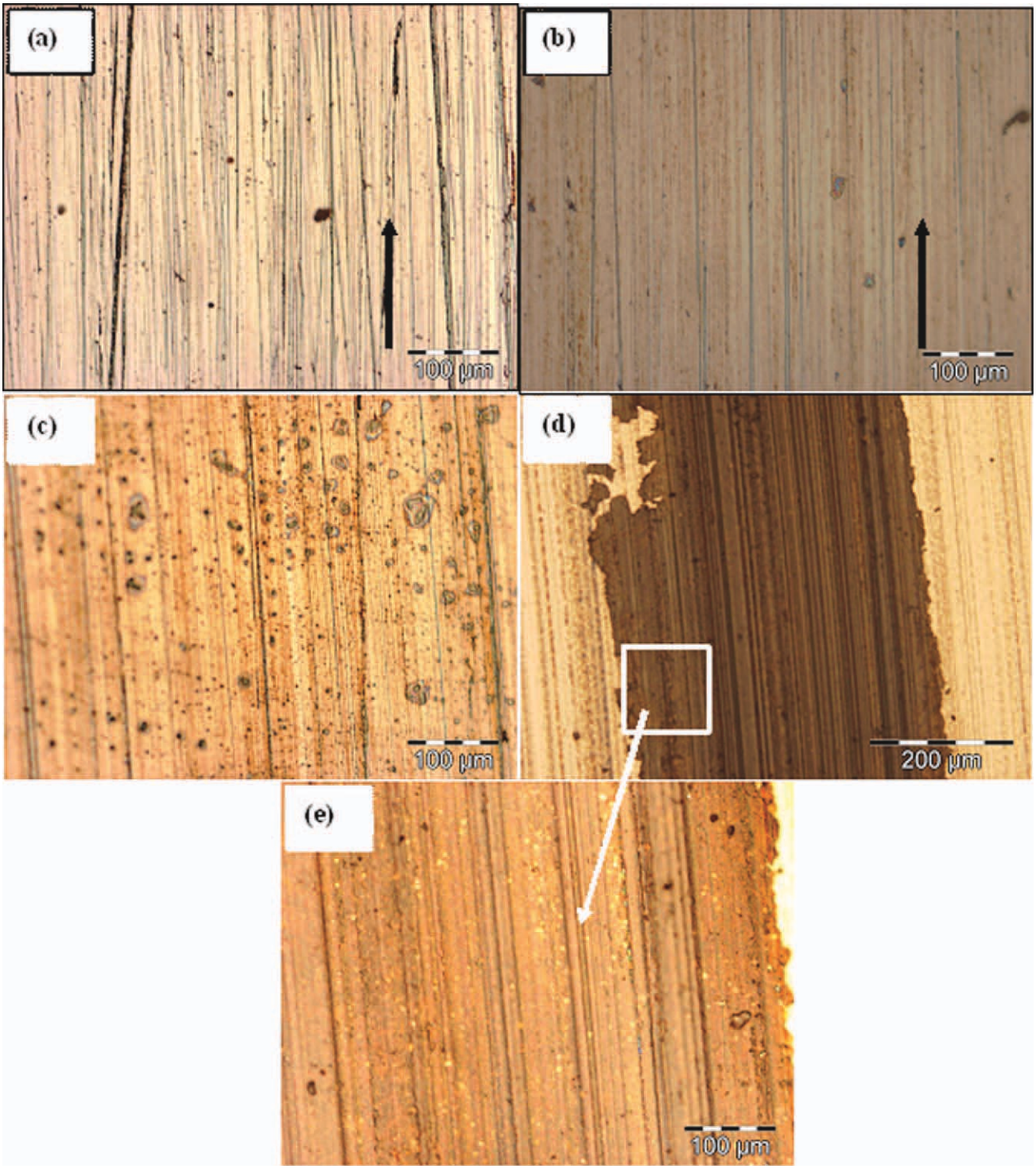


**Figure 5** Optical micrographs of transfer films developed on steel countersurface during sliding wear for (a) as polished countersurface, (b) ANM-0 (PEEK), (c) ANM-20, and (d and e) ANM-50. Arrow shows sliding direction (sliding speed: 1 m/s and sliding distance: 3 km). [Color figure can be viewed in the online issue, which is available at wileyonlinelibrary.com.]

### SEM study of worn surfaces

The SEM images of the debris of pure PEEK, 30 wt % (ANM-30) microcomposite and MS are shown in Figure 6(a–c), respectively. The wear of PEEK generates flaky or lamellae like debris on the steel countersurface during wearing because the debris can be easily removed during subsequent wear. The size of ANM-30 microcomposite debris is smaller than that of pure PEEK. As the AlN content in PEEK increases debris particle size decreases. Figure 6(c) shows that

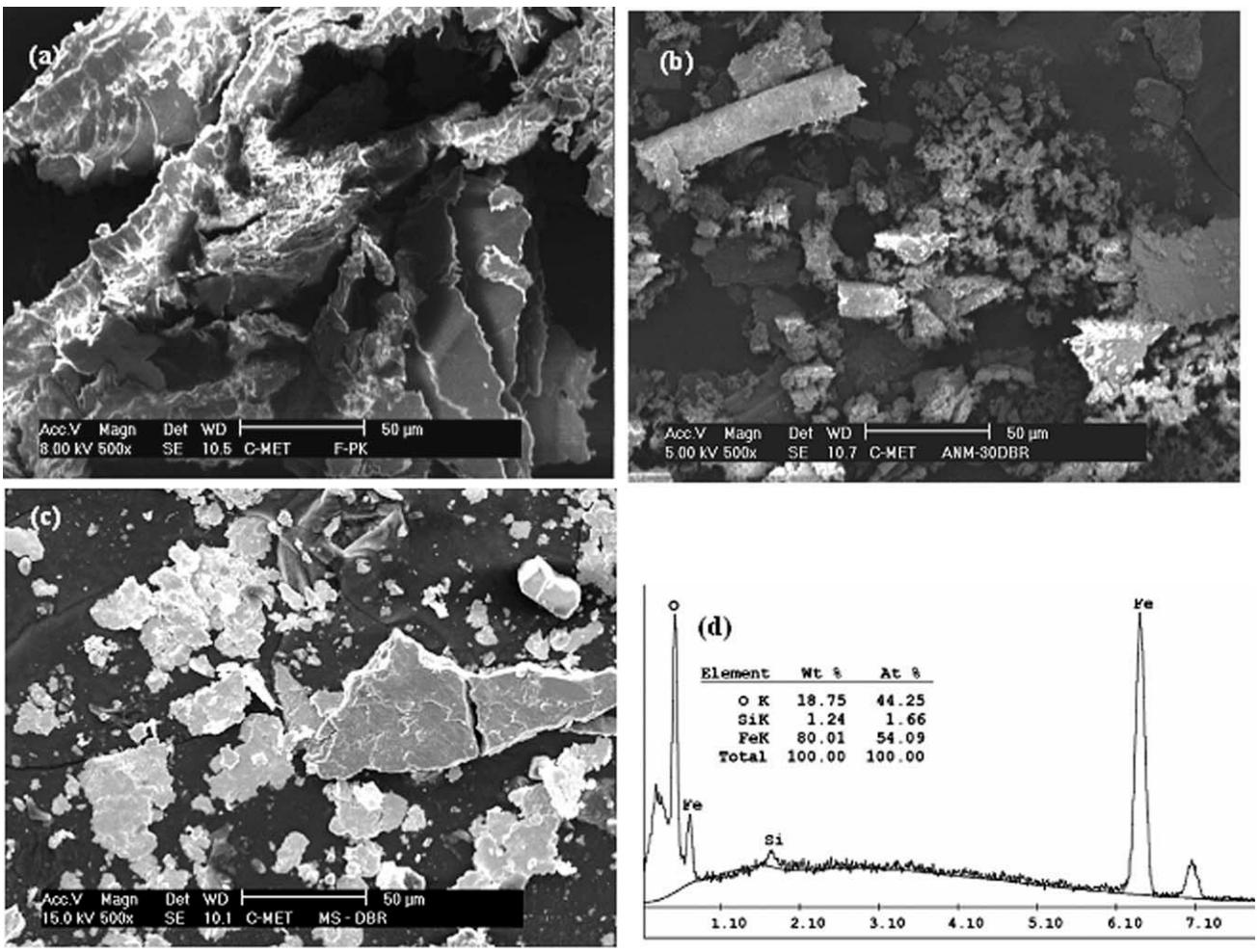


**Figure 6** SEM of debris of (a) ANM-0, (b) ANM-30, (c) mild steel (scale bar: 50 μm), and (d) EDS of debris of mild steel.

the size of wear debris generated by MS is from several microns to more than 50 μm and debris have sharp edges, which probably result in much higher wear rate of MS than that of pure PEEK and its composites. Figure 6(d) shows EDS of debris of MS. We can clearly see that there are two most strong peaks indicating presence of oxygen and iron, i.e., formation of iron oxide during repeated dry sliding.

Figure 7 shows SEM images of the worn surfaces of the pure PEEK and its microcomposites. The worn surface of pure PEEK shows a sign of adhesive wear as shown in Figure 7(a,b), which was caused by the removal of flaky or lamellae like debris from the pure PEEK surface. This indicates that adhesion is the dominant wear mechanism for pure PEEK. In contrast, ANM-20 microcomposite shows adhesive and microploughing wear as shown in Figure 7(c,d). Figure 7(e) showing the worn surface of ANM-50 also indicates adhesive wear with sign of microploughing. It is obvious that in this case the adhesive film is quite discontinuous/patchy. Thus, AlN particles present in the composite pin are exposed, which can be clearly seen at higher magnification in Figure 7(f). The worn surface of ANM-50 also contains wear particles originating from the steel countersurface. To confirm this, EDS was conducted on the worn surface of ANM-50 composite pin. The EDS spectrum shows presence of Al (from AlN), Fe and Mo elements (from EN-24 steel countersurface). This reveals that AlN along with PEEK and metallic particles containing Fe/Mo are transferred from the composite pin and countersurface, respectively to form a mechanically mixed layer on the composite pin. Thus, SEM and EDS examination of worn PEEK/AlN composites indicates that higher loading of micro-AlN in the composites can cause three phenomena named as adhesive film becomes discontinuous, microploughing mechanism becomes operative due to third body abrasion resulting from hard particles (AlN and steel) in the debris, and even hard countersurface also gets damaged generating metallic particles. Figure 8 shows SEM image of worn surface of the 30 wt % nano-AlN (ANN-30) nanocomposite. This shows that adhesive wear is almost abated. Hence, wear rate of the nanocomposites is decreased significantly.

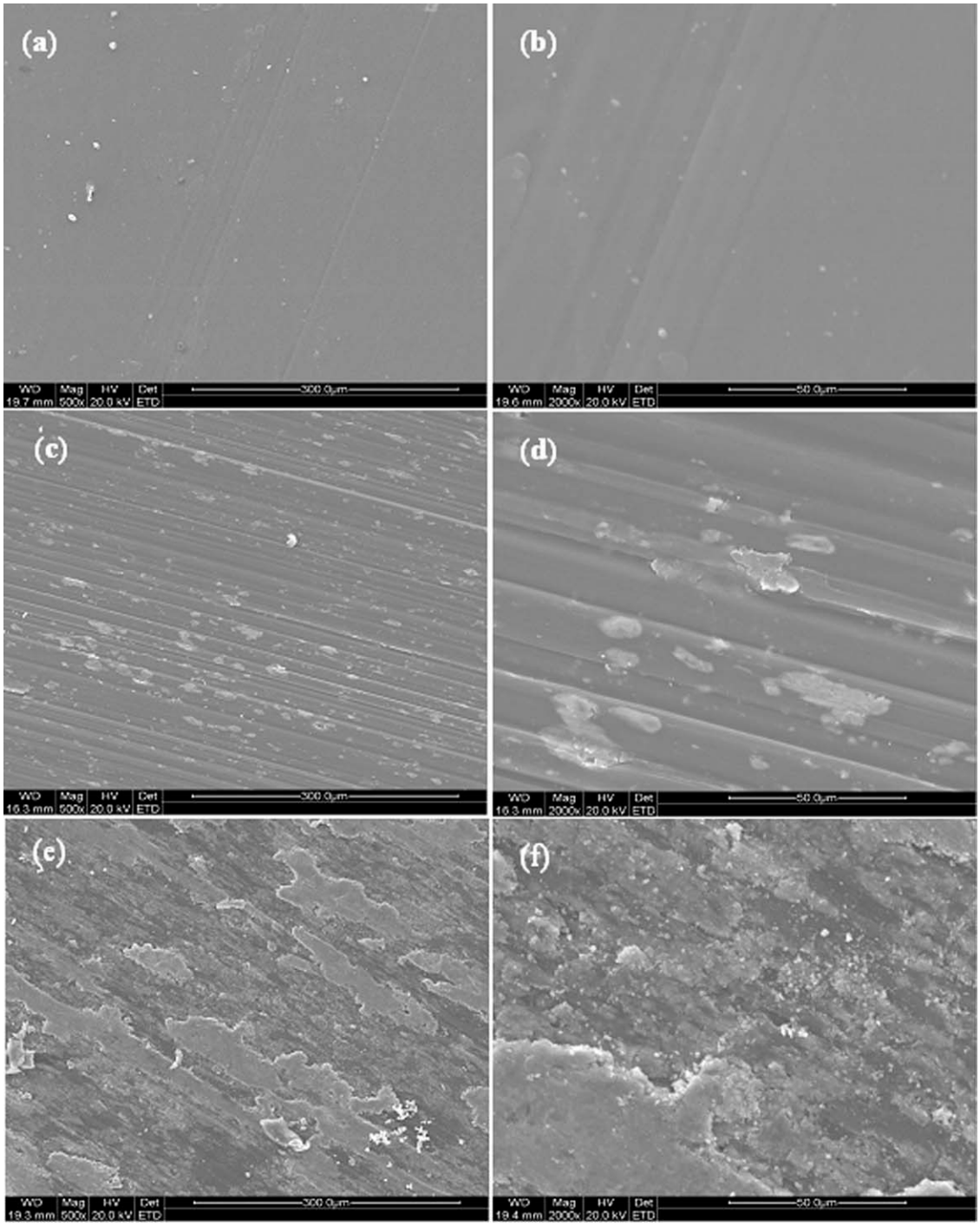


**Figure 7** SEM of worn surface of (a and b) ANM-0, (c and d) ANM-20, and (e and f) ANM-50 [scale bar: 300 μm (for a, c, and e) and 50 μm (for b, d, and f)]

## CONCLUSIONS

On the basis of the above investigations, the following conclusions can be drawn.

1. Wear resistance (i.e., inverse of specific wear rate) of PEEK sliding against EN-24 steel countersurface is increased by about 2-fold at 20 wt % micro-AlN and by more than 4-fold at 30 wt % nano-AlN content. The significant improvement in wear resistance is attributed to the formation of a thin and coherent transfer film between the composite pin and countersurface.
2. Wear resistant of PEEK/AlN microcomposite containing above 30 wt % AlN decreases with increasing AlN. This is attributed to the poor

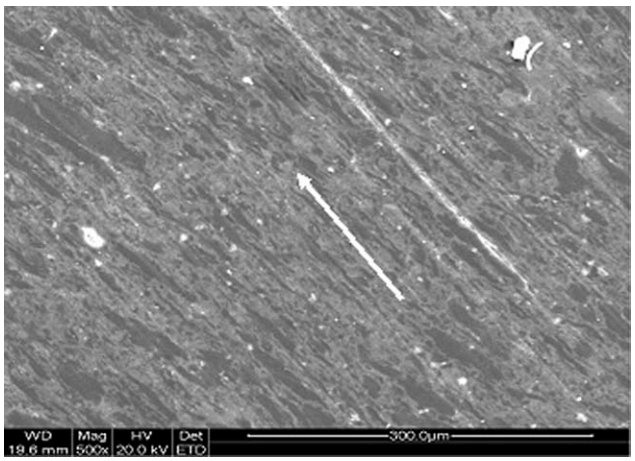


**Figure 8** SEM of worn surface of ANN-30 (scale bar: 300 μm; arrow shows sliding direction).

quality transfer film and third body wear mechanism.

3. Coefficient of friction of microcomposites is higher than that of pure PEEK. However, it is lower for nanocomposites at smaller load than pure PEEK.

## References

1. Goyal, R. K.; Tiwari, A. N.; Negi, Y. S. Eur Polym J 2005, 41, 2034.
2. Goyal, R. K.; Tiwari, A. N.; Mulik, U. P.; Negi, Y. S. Compos Part A 2007, 38, 516.
3. Kurokawa, M.; Uchiyama, Y.; Nagai, S. Tribol Int 2000, 33, 715.
4. Yamamoto, Y.; Hashimoto, M. Wear 2004, 257, 181.
5. Friedrich, K.; Zhang, Z.; Schlarb, A. K. Compos Sci Technol 2005, 65, 2329.
6. Kurokawa, M.; Uchiyama, Y.; Nagai, S. Tribol Int 1999, 32, 491.
7. Zhang, R.; Häger, A. M.; Friedrich, K.; Song, Q.; Dong, Q. Wear 1995, 181–183, 613.
8. Zhang, Z.-Z.; Xue, Q. J.; Liu, W.-M.; Shen, W.-C. Wear 1997, 210, 151.
9. Bahadur, S.; Sunkara, C. Wear 2005, 258, 1411.
10. Briscoe, B. Tribol Int 1981, 14, 231.
11. Bahadur, S.; Gong, D. Wear 1992, 154, 151.
12. Lancaster, J. K. Tribol Int 1972, 5, 249.
13. Bahadur, S.; Gong, D.; Anderegg, J. W. Wear 1993, 160, 1381.
14. Wang, Q. H.; Xu, J.; Shen, W.; Liu, W. Wear 1996, 196, 82.
15. Wang, Q.; Xue, Q.; Shen, W. Tribol Int 1997, 30, 193.
16. Sawyer, W. G.; Freudenberg, K. D.; Bhimaraj, P.; Schadler, S. Wear 2003, 254, 573.
17. Li, F.; Hu, K.; Li, J.; Zhao, B. Wear 2002, 249, 877.
18. Rong, M. Z.; Zhang, M. G.; Liu, H.Zeng, H. M.; Werzel, B.; Friedrich, K. Ind Lubric Tribol 2001, 53, 72.
19. Durand, J. M.; Vardavouliar, M.; Jeandin, M. Wear 1995, 181–183, 833.
20. Schwartz, C. J.; Bahadur, S. Wear 2000, 237, 261.
21. Bhimaraj, P.; Burris, D. L.; Action, J.; Sawyer, W. G.; Toney, C. G.; Siegel, R. W.; Schadler, L. S. Wear 2005, 258, 1437.
22. Qiao, H.-B.; Guo, Q.; Tian, A.-G.; Pan, G.-L.; Xu, L.-B. Tribol Int 2007, 40, 105.
23. Frederic, N. C. Thermoplastic Aromatic Polymer Composites; Butterworth Heinemann Ltd.: Oxford, 1992.
24. Lu, Z. P.; Friedrich, K. Wear 1995, 181–183, 624.
25. Werner, P.; Altstädt, V.; Jaskulka, R.; Jacobs, Q.; Sandler, J. K. B.; Shaffler, M. S. P.; Windle, A. H. Wear 2004, 257, 1006.
26. Hanchi, J.; Eiss, N. S., Jr. Wear 1997, 203–204, 380.
27. Wang, Q. H.; Xu, J.; Shen, W.; Xue, Q. Wear 1997, 209, 316.
28. Wang, Q. H.; Xu, J.; Liu, H.; Shen, W.; Xu, J. Wear 1996, 198, 216.
29. Goyal, R. K.; Tiwari, A. N.; Mulik, U. P.; Negi, Y. S. J Nanosci Nanotechnol 2009, 9, 6902.
30. Kume, S.; Yasuoka.M.; Omura, N.; Watari, K.; J Am Ceram Soc 2005, 88, 3229.
31. Goyal, R. K.; Tiwari, A. N.; Negi, Y. S. Mater Sci Eng A 2008, 486, 602.